

Coercivity and microstructure of sintered Nd-Fe-B magnets diffused with Pr-Co, Pr-Al, and Pr-Co-Al alloys

Lei Jin(金磊), Zhe-Huan Jin(金哲欢), Jin-Hao Zhu(朱金豪), Guang-Fei Ding(丁广飞), Bo Zheng(郑波) , Shuai Guo(郭帅), Ren-Jie Chen(陈仁杰), A-Ru Yan(闫阿儒), and Xin-Cai Liu(刘新才)

Citation: Chin. Phys. B, 2021, 30 (**2**): 027503. DOI: 10.1088/1674-1056/abc166
Journal homepage: http://cpb.iphy.ac.cn; http://iopscience.iop.org/cpb

What follows is a list of articles you may be interested in

Effect of annealing temperature on coercivity of Nd-Fe-B magnets with TbFeAl doping by process of hot-pressing

Ze-Teng Shu(舒泽腾), Bo Zheng(郑波), Guang-Fei Ding(丁广飞), Shi-Cong Liao(廖是聪), Jing-Hui Di(邸敬慧), Shuai Guo(郭帅), Ren-Jie Chen(陈仁杰), A-Ru Yan(闫阿儒), Lei Shi(石磊)
Chin. Phys. B, 2020, 29 (**5**): 057501. DOI: 10.1088/1674-1056/ab7b57

Grain boundary restructuring and La/Ce/Y application in Nd-Fe-B magnets

Mi Yan(严密), Jiaying Jin(金佳莹), Tianyu Ma(马天宇)
Chin. Phys. B, 2019, 28 (**7**): 077507. DOI: 10.1088/1674-1056/28/7/077507

Progress in recycling of Nd-Fe-B sintered magnet wastes

Ming Yue(岳明), Xiaowen Yin(尹小文), Weiqiang Liu(刘卫强), Qingmei Lu(路清梅)
Chin. Phys. B, 2019, 28 (**7**): 077506. DOI: 10.1088/1674-1056/28/7/077506

Regulating element distribution to improve magnetic properties of sintered Nd-Fe-B/Tb-Fe-B composite magnets

Zhu-Bai Li(李柱柏), Jing-Yan Zuo(左敬燕), Dong-Shan Wang(王东山), Fei Liu(刘飞), Xue-Feng Zhang(张雪峰)
Chin. Phys. B, 2019, 28 (**7**): 077503. DOI: 10.1088/1674-1056/28/7/077503

Magnetic properties of misch-metal partially substituted Nd-Fe-B magnets sintered by dual alloy method

Jie-Fu Xiong(熊杰夫), Rong-Xiang Shang(商荣翔), Yan-Li Liu(刘艳丽), Xin Zhao(赵鑫), Wen-Liang Zuo(左文亮), Feng-Xia Hu(胡凤霞), Ji-Rong Sun(孙继荣), Tong-Yun Zhao(赵同云), Ren-Jie Chen(陈仁杰), Bao-Gen Shen(沈保根)
Chin. Phys. B, 2018, 27 (**7**): 077504. DOI: 10.1088/1674-1056/27/7/077504

Coercivity and microstructure of sintered Nd–Fe–B magnets diffused with Pr–Co, Pr–Al, and Pr–Co–Al alloys*

Lei Jin(金磊)[1,2], Zhe-Huan Jin(金哲欢)[1,2], Jin-Hao Zhu(朱金豪)[2], Guang-Fei Ding(丁广飞)[2], Bo Zheng(郑波)[2], Shuai Guo(郭帅)[2,3,†], Ren-Jie Chen(陈仁杰)[2,3], A-Ru Yan(闫阿儒)[2,3], and Xin-Cai Liu(刘新才)[1,‡]

[1] *School of Materials Science and Chemical Engineering, Ningbo University, Ningbo* 315211, *China*

[2] *Key Laboratory of Magnetic Materials and Devices, Ningbo Institute of Materials Technology and Engineering, Chinese Academy of Sciences, Ningbo* 315201, *China*

[3] *University of Chinese Academy of Sciences, Beijing* 100049, *China*

(Received 27 August 2020; revised manuscript received 26 September 2020; accepted manuscript online 15 October 2020)

The commercial 42M Nd–Fe–B magnet was treated by grain boundary diffusion (GBD) with $Pr_{70}Co_{30}$ (PC), $Pr_{70}Al_{30}$ (PA) and $Pr_{70}Co_{15}Al_{15}$ (PCA) alloys, respectively. The mechanism of coercivity enhancement in the GBD magnets was investigated. The coercivity was enhanced from 1.63 T to 2.15 T in the PCA GBD magnet, higher than the 1.81 T of the PC GBD magnet and the 2.01 T of the PA GBD magnet. This indicates that the joint addition of Co and Al in the diffusion source can further improve the coercivity. Microstructural investigations show that the coercivity enhancement is mainly attributed to the exchange-decoupling of the GB phases. In the PCA GBD magnet, the wider thin GB phases can be formed and the thin GB phases can still be observed at the diffusion depth of 1500 μm due to the combined action of Co and Al. At the same time, the formation of the Pr-rich shell can also be observed, which is helpful for the coercivity enhancement.

Keywords: Nd–Fe–B, coercivity, Pr–Co–Al alloys, grain boundary diffusion

PACS: 75.60.Nt, 75.50.Ww, 75.50.Vv, 75.60.Ej **DOI:** 10.1088/1674-1056/abc166

1. Introduction

Sintered Nd–Fe–B permanent magnets have a wide range of applications due to their excellent magnetic properties at room temperature. However, their magnetic properties deteriorate seriously at high temperatures due to poor thermal stability. This limits their application in some fields such as the traction motors of hybrid electric vehicles and wind generators.[1,2] Thus, it is necessary to improve the coercivity of Nd–Fe–B magnets. A common method for coercivity enhancement is to form $(Nd,Tb/Dy)_2Fe_{14}B$ grains of higher anisotropy field H_A through addition of heavy rare earth (HRE) (e.g., Tb and Dy) in Nd–Fe–B alloys.[3,4] However, this way may result in reduction of remanence due to anti-ferromagnetic coupling between Fe and HRE.[5] In recent years, the increase of Tb/Dy price leads to an increase in the cost. Therefore, the grain boundary diffusion (GBD) process has attracted more and more attention. In this method, the consumption of HRE is limited, the matter containing HRE coated on the magnet surface is diffused into the magnet along the grain boundary (GB) through the heat treatment, to form the HRE-rich shell with a higher H_A and thin GB phases. The main reason for the coercivity enhancement is the magnetic hardening effect of the HRE-rich shell and the exchange-decoupling of the GB phases.[6,7]

Recently, in order to save Tb/Dy resources, the coercivity enhancement by GBD with HRE-free diffusion source has successfully applied to the sintered Nd–Fe–B magnets, such as Pr–Al–Cu, Pr–Cu and $Nd_{70}Cu_{30}$.[8–10] The coercivity enhancement of the HRE-free diffusion source GBD magnets is mainly attributed to the formation of continuous GB phases. This can effectively improve the exchange-decoupling between adjacent grains.[1,11–15] The HRE-free diffusion source is mainly composed of light rare earth (LRE) phase and non-rare earth phase. In order to obtain higher coercivity, the LRE phase usually chooses Pr because the H_A of $Pr_2Fe_{14}B$ is higher than that of $Nd_2Fe_{14}B$.[4] The choice of non-rare earth elements is also crucial. Because the main function of non-rare earth elements is to promote GBD and the formation of continuous GB phases. Al has been widely used in diffusion sources because it can effectively improve the wettability of GB phase.[6,16,17] In the preparation of Nd–Fe–B alloy, a small amount of Co is usually added to improve the magnetic properties.[18–21] Chen *et al.*[22] reported that the coercivity and remanence at high temperatures can be increased simultaneously due to the formation of the Dy and Co enriched shell structure, when the commercial sintered Nd–Fe–B magnet diffused with $Dy_{60}Co_{40}$ alloy. In addition, Lee *et al.*[23] reported that the coercivity of magnets can be further enhanced

*Project supported by the Key Research and Development Program of Zhejiang Province, China (Grant No. 2021C01190), the Major Project of Science and Technology Innovation 2025 in Ningbo City, China (Grant No. 2018B10015), Zhejiang Province Public Welfare Technology Application Research Project (Grant No. LGG21E010007), the Inner Mongolia Major Technology Project, and the K. C. Wong Magna Fund in Ningbo University.

†Corresponding author. E-mail: gshuai@nimte.ac.cn

‡Corresponding author. E-mail: liuxincai@nbu.edu.cn

© 2021 Chinese Physical Society and IOP Publishing Ltd

when the mixed powder of DyCo and Al is used as the diffusion sources. This indicates that the addition of Co and Al in the diffusion source is helpful for the coercivity enhancement. Thus, in order to achieve the coercivity enhancement through the HRE-free diffusion source GBD, we design $Pr_{70}Co_{30}$ (PC), $Pr_{70}Al_{30}$ (PA) and $Pr_{70}Co_{15}Al_{15}$ (PCA) diffusion sources and conduct GBD for the commercial 42M Nd–Fe–B magnet. In this work, the mechanism of coercivity enhancement in the GBD magnets and the effects of Co and Al on the magnetic properties are investigated based on the microstructural observation.

2. Experimental details

The commercial 42M sintered Nd–Fe–B magnet of size 6 mm × 6 mm × 5 mm were used as the original sample. $Pr_{70}Co_{30}$ (at%), $Pr_{70}Al_{30}$ (at%) and $Pr_{70}Co_{15}Al_{15}$ (at%) alloys were prepared by arc-melting with industry raw materials Pr, Co and Al in high purity argon atmosphere. These alloys are cut into sheets in dimensions of 6 mm × 6 mm × 0.2 mm (thickness) with wire-electrode cutting. These sheets are ground to the same mass through abrasive papers in alcohol and then used as diffusion sources. The original magnet is located between two sheets and placed in a high temperature resistant mold, in which the interface between the magnet and the sheet is perpendicular to the *c*-axis. Finally, these samples were performed in the diffusion treatment at 800 °C for 10 h and annealed at 500 °C for 2 h. The magnetic properties were measured by pulsed field magnetometer (PFM14.CN). The microstructure, element concentration and elemental distribution were analyzed by scanning electron microscopy (SEM, FEI Quanta FEG 250) and energy-dispersive x-ray spectrometry (EDS). The local microstructure and elemental distribution were examined by a Talos F200X scanning/transmission electron microscope (S/TEM).

3. Results and discussion

Figure 1 shows the demagnetization curves of the original and GBD processed magnets by PC, PA and PCA alloys at 20 ℃. After diffusing treatment, the coercivity increase from original 1.63 T to 1.81 T, 2.01 T and 2.15 T, respectively. The remanence reduced from 1.34 T to 1.33 T, 1.28 T and 1.30 T, respectively. It can be seen that the coercivity enhancement of the PA GBD magnet is better than that of the PC GBD magnet. However, the coercivity enhancement of the PCA GBD magnet is most outstanding, reaching 0.52 T. This indicates that the alone addition of Al in the diffuser source is better than that of Co for the coercivity enhancement, while the joint addition of Co and Al in the diffusion source can further improve the coercivity. Moreover, it can be found that the decline of remanence is significantly reduced when Co is added to the diffusion source. In order to further analyze the mechanism of coercivity enhancement in the GBD magnets, the microstructure of the magnets after diffusion was observed.

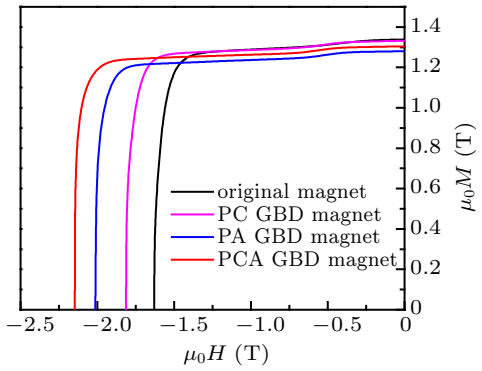


Fig. 1. Demagnetization curves of the original magnet and the PC, PA and PCA GBD magnets.

Figure 2 shows backscattered electron (BSE) SEM images of magnets by the PC, PA and PCA alloys' diffusion at different depths from the surface of magnets, respectively. In the PC GBD magnet, the GB phases are mainly concentrated in the triple junctions. However, in the PA and PCA GBD magnets, the continuous GB phases (also known as the thin GB phases) with bright area in the SEM images can be clearly observed and uniformly distributed around the $Nd_2Fe_{14}B$ grain with black area. This structure can effectively enhance the coercivity by reducing the exchange interaction of the adjacent grains.[1,11–13] It is worth noting that the continuous GB phases of the PCA GBD magnet is obviously wider than that of the PA GBD magnet at the same diffusion depth. In addition, the range of continuous GB phases is significantly deeper in the PCA GBD magnets. When the diffusion depth reaches 1200 μm, the continuous GB phases are almost invisible in the PA GBD magnet. In the PCA GBD magnet, even at 1500 μm, the continuous GB phases can still be observed. This indicates that the alone addition of Co in the diffusion source cannot improve the continuity of GB phases, while Al can effectively improve the continuity of GB phases. However, the joint addition of Al and Co in the diffusion source can further promote the formation of continuous GB phases. Therefore, the coercivity of the PCA GBD magnet is higher than that of the PA GBD magnet, while the PC GBD magnet has the lowest coercivity.

Figure 3 shows the SEM images and the EDS mapping images of the PC, PA and PCA GBD magnets at 50 μm from the surfaces close to the diffusion sources. In the PC GBD magnet, Pr and Co are mainly concentrated in the triple junction phases. In the outermost layer of the $Nd_2Fe_{14}B$ grain, the Co-rich shells can be observed. However, in the PA GBD magnet, Pr is continuously distributed along the thin GB and presented a network structure surrounding the $Nd_2Fe_{14}B$ grain.

Al can also be observed at the thin GB phases and not concentrated in the triple junction phases like Co. It should be noted that the Al concentration in the outermost layer of the $Nd_2Fe_{14}B$ grain is higher than that in the nearby GB, the Al-rich shells can also be observed. This indicates that Al can improve the wettability of GB phases and promote Pr in the triple junctions flowing into the thin GB to form the continuous GB phases. Co cannot effectively improve the wettability of GB phases, so that Pr is mainly concentrated in the triple junctions. In addition, both Co and Al easily enter the $Nd_2Fe_{14}B$ grain and form the shells. However, the small addition of Co in the sintered $Nd_2Fe_{14}B$ can improve the remanence.[18,19] Therefore, the decline of remanence is the lowest in the PC GBD magnet.

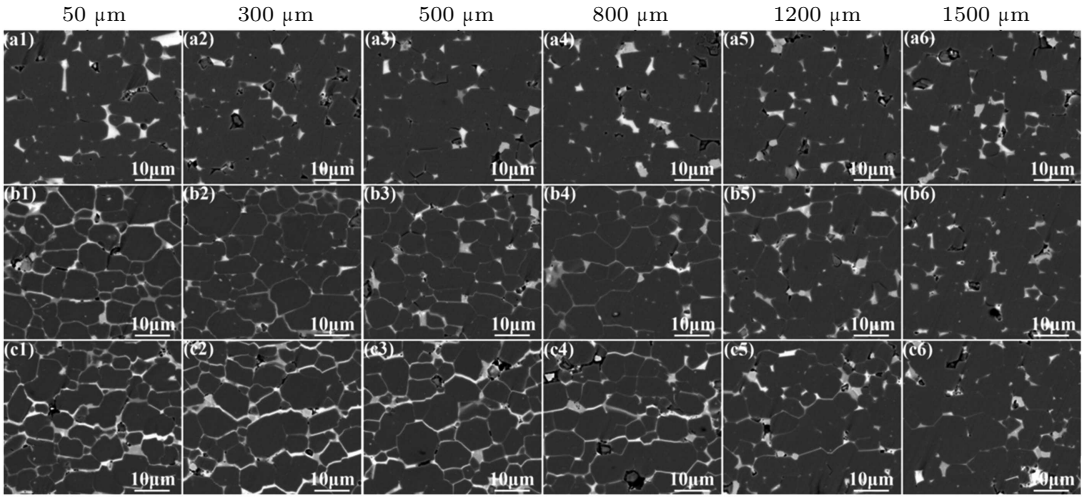


Fig. 2. BSE-SEM images of the PC GBD magnet [(a1) 50 μm, (a2) 300 μm, (a3) 500 μm, (a4) 800 μm, (a5) 1200 μm, (a6) 1500 μm], PA GBD magnet [(b1) 50 μm, (b2) 300 μm, (b3) 500 μm, (b4) 800 μm, (b5) 1200 μm, (b6) 1500 μm], and PCA GBD magnet [(c1) 50 μm, (c2) 300 μm, (c3) 500 μm, (c4) 800 μm, (c5) 1200 μm, (c6) 1500 μm] at different depths from the diffused surface of magnet.

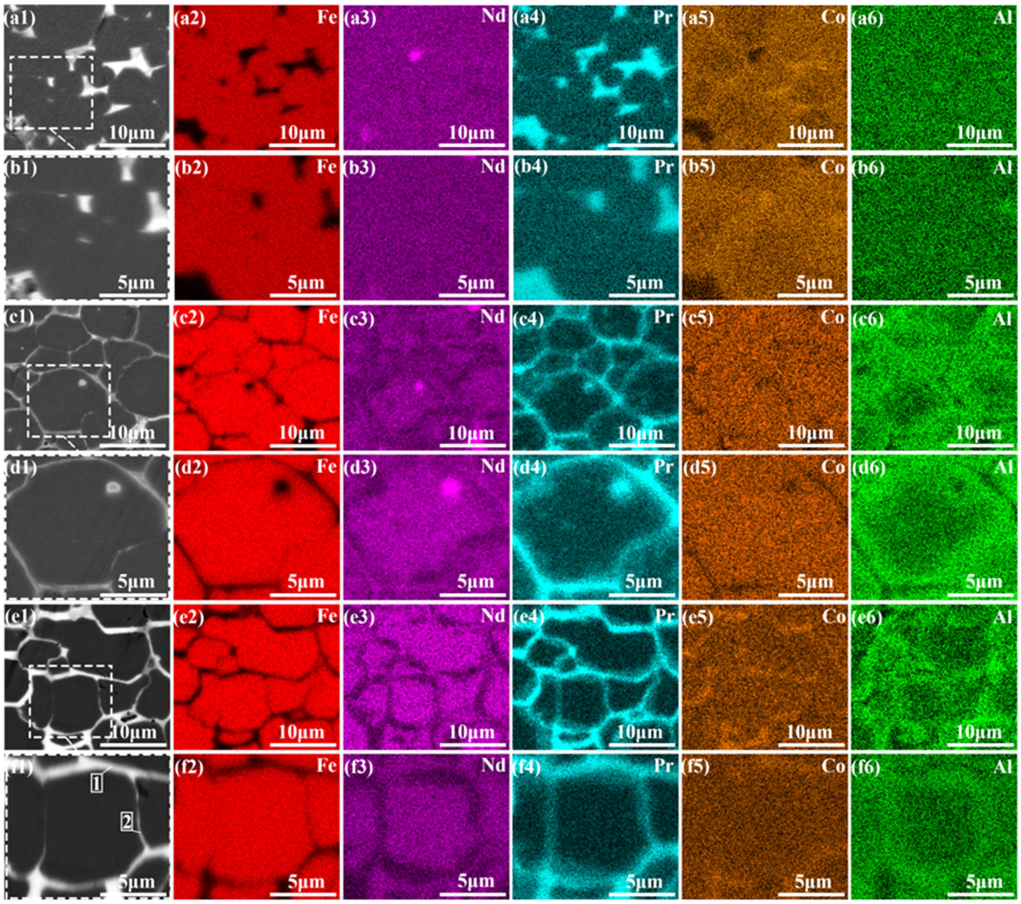


Fig. 3. BSE-SEM images and EDS mapping images of the PC GBD magnet [(a1)–(a6), (b1)–(b6)], the PA GBD magnet [(c1)–(c6), (d1)–(d6)], and the PCA GBD magnet [(e1)–(e6), (f1)–(f6)] at 50 μm from the diffused surface.

It is noted that Pr is also continuously distributed along the thin GB and presented a network structure in the PCA GBD magnet. However, the Pr concentration at the thin GB phases is obviously higher than that in the PA GBD magnet. This suggests that the joint addition of Al and Co in the diffusion source can make more Pr infiltrate into the thin GB to form the thin GB phases. Figure 4 is the concentration distribution of Pr in the GBD magnets with the increase of diffusion depth. In order to determine the concentration at different diffusion depths, we select a series of 100 μm × 100 μm areas at 50–1850 μm from the diffused surface and calculate qualitatively the concentration of Pr for each area by EDS. Within the diffusion depth of 50–1250 μm, it is noted that the PCA GBD magnet has the highest Pr concentration, the Pr concentration in the PA GBD magnet is second, while the Pr concentration is lowest in the PC GBD magnet. This indicates that the diffusion effect of Al on Pr is better than that of Co, while the joint addition of Al and Co in the diffusion source can further promote Pr diffusion into the magnet. Thus, in the PCA GBD magnet, a wide range of continuous GB phases can be formed and the width of the thin GB phases is also wider. In order to further analyze the effect of Co and Al on Pr in the GBD, the element distribution of the diffused magnet is characterized by TEM.

Figure 5 shows the HAADF-STEM images of the PC, PA and PCA GBD magnets near the diffused surface, respectively. It can be found that Pr is mainly concentrated in the triple junction phases and only a few parts are distributed in the thin GB phases in the PC GBD magnet. However, in the PA and PCA GBD magnets, Pr exists extensively at the triple junction phases and the thin GB phases. This indicates that the wettability of GB phases in the PA and PCA GBD magnets is better than that of the PC GBD magnets. Through the distribution of Co and Al, it can be observed that Co is mainly concentrated in the triple junction phases and the distribution at the thin GB phases is not obvious in the PC GBD magnet. In the PA GBD magnet, Al is distributed at the triple junction phases and the thin GB phases. Co can be observed in the PA GBD magnet due to the presence of Co in the commercial 42M sintered Nd–Fe–B magnet. However, in the PA GBD magnet, the change of the magnet structure after diffusion is mainly caused by the Pr and Al in the diffusion source. Through the comparison between the PC GBD magnet and the PA GBD magnet, it can also be inferred that the wettability of GB phases cannot be effectively improved by Co, whereas can be effectively improved by Al.

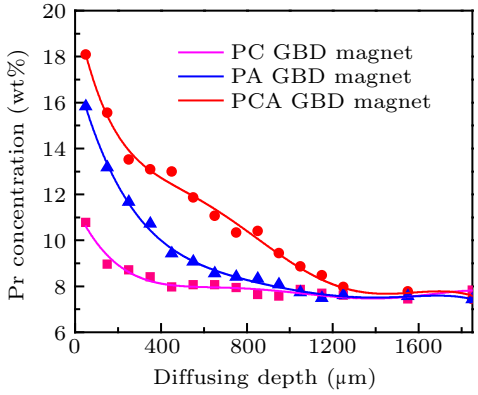


Fig. 4. The concentration distribution of Pr in the PC, PA and PCA GBD magnets with the increase of diffusion depth from the diffused surface.

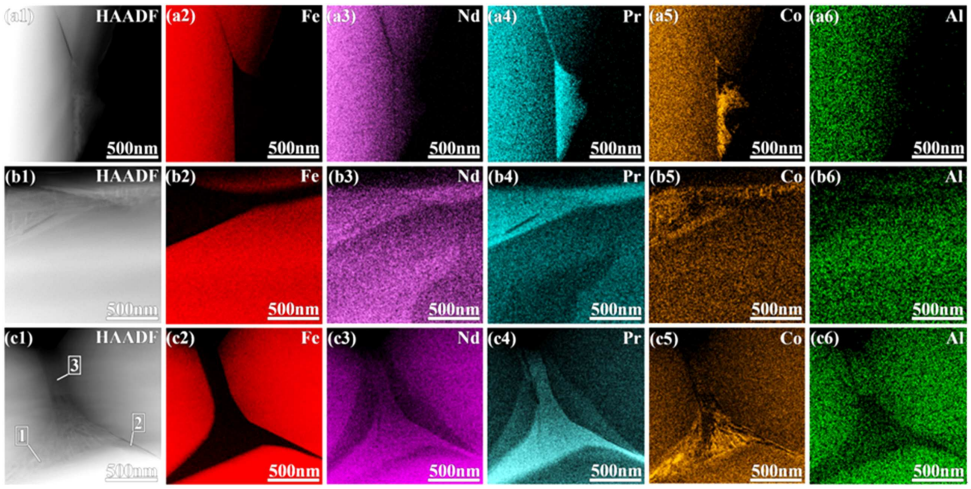


Fig. 5. The HAADF-STEM images of the PC GBD magnet (a1)–(a6), the PA GBD magnet (b1)–(b6) and the PCA GBD magnet (c1)–(c6) near the diffused surface.

In the PCA GBD magnet, there are three kinds of the thin GB phases (1, 2 and 3), as shown in Fig. 5(c1). Compared with the thin GB phase 3, the content of Pr and Co is higher and the content of Al is lower in the thin GB phases 1 and 2. This phenomenon can also be observed in Figs. 3(e1)–3(e6) and 3(f1)–3(f6). As shown in Fig. 3(f1), there are two kinds of the thin GB phases (1 and 2) in the PCA GBD magnet. The width of the thin GB phases 1 is obviously wider than that of

the thin GB phases 2. Compared with the thin GB phases 2, the character of element distribution in the thin GB phases 1 is rich-Pr, rich-Co and poor-Al. However, Co has been shown to be unable to effectively enhance the the wettability of GB phases through the PC GBD magnet, the improvement of GB phases wettability mainly depends on Al. However, the width of the thin GB phases in the PA GBD magnet is obviously narrower than that in the PCA GBD magnet. This indicates that the formation of the wider thin GB phases in the PCA GBD magnet is the combined action of Co and Al. It can be inferred that, in the PCA diffusion sources, the main effect of Al is to improve the wettability of the GB phases, while the addition of Co can further improve the fluidity of Pr, so that more Pr flows into the thin GB from the triple junctions and then forms the wider thin GB phases.

In addition, it can be found that the Pr concentration at the outermost layer of the $Nd_2Fe_{14}B$ grain is significantly higher than that at the grain inner in the PA and PCA GBD magnets from Figs. 3(c4), 4(d4), 4(e4), 4(f4) and Figs. 5(b4) and 5(c4). In the outermost layer of the $Nd_2Fe_{14}B$ grain, the Nd concentration is obviously lower than that of the grain inner. This indicates that the Pr-rich shells are formed in the PA and PCA GBD magnets. The effect of the Pr-rich shell on the magnetic properties of the Nd–Fe–B magnet[8,24,25] has been reported, which can further improve the coercivity of magnet because the H_A of the $Pr_2Fe_{14}B$ is higher than that of $Nd_2Fe_{14}B$.[4] Through micromagnetic simulation, Oikawa *et al.*[26] have shown that the Nd–Fe–B magnet with Pr-rich shells has a higher coercivity at 27°C. Thus, the existence of the Pr-rich shells in the PA and PCA GBD magnets is also helpful for the coercivity enhancement.

4. Conclusions

The magnetic properties and microstructure have been investigated in the sintered Nd–Fe–B magnet by grain boundary diffusion with $Pr_{70}Co_{30}$, $Pr_{70}Al_{30}$ and $Pr_{70}Co_{15}Al_{15}$ alloys, respectively. The coercivity is enhanced from 1.63 T to 1.81 T, 2.01 T and 2.15 T by grain boundary diffusion with $Pr_{70}Co_{30}$, $Pr_{70}Al_{30}$ and $Pr_{70}Co_{15}Al_{15}$ alloys, respectively. The microstructure analysis shows that Al can effectively improve the wettability of GB phases, while Co can further improve the fluidity of Pr. Thus, when $Pr_{70}Co_{15}Al_{15}$ alloy is used as a diffusion source, more Pr can diffuse into the magnet to form the wider thin GB phases, and the depth of continuous GB phases is also enhanced. This results in the obvious coercivity enhancement in the $Pr_{70}Co_{15}Al_{15}$ GBD magnet, mainly due to fact that the exchange-decoupling effect is obviously strengthened. The Pr-rich shell is also helpful for the coercivity enhancement. In addition, the addition of Co in the diffusion source inhibits the deterioration of remanence to a certain extent. In general, in the GBD process, the magnetic properties of the sintered Nd–Fe–B magnet can be effectively improved when $Pr_{70}Co_{15}Al_{15}$ alloy is used as the diffusion source, which provides a certain reference for the subsequent diffusion source design.

References

[1] Hono K and Sepehri-Amin H 2012 *Scr. Mater* **67** 530
[2] Brown D, Ma B M and Chen Z M. 2002 *J. Magn. Magn. Mater.* **248** 432
[3] Gutfleisch O, Willard M A, Bruck E, Chen C H, Sankar S G and Liu J P 2011 *Adv. Mater.* **23** 821
[4] Hirosawa S, Matsuura Y, Yamamoto H, Fujimura S, Sagawa M and Yamauchi H 1986 *J. Appl. Phys.* **59** 873
[5] Herbst J F 1991 *Rev. Mod. Phys.* **63** 819
[6] Di J H, Ding G F, Tang X, Yang X, Guo S, Chen R J and Yan A R 2018 *Scr. Mater.* **155** 50
[7] Sepehri-Amin H, Ohkubo T and Hono K 2013 *Acta Mater.* **61** 1982
[8] Zeng H X, Liu Z W, Li W, Zhang J S, Zhao L Z, Zhong X C, Yu H Y and Guo B C 2019 *J. Magn. Magn. Mater.* **471** 97
[9] Chen F G, Zhang T Q, Wang J, Zhang L T and Zhou G F 2015 *Scr. Mater.* **107** 38
[10] Tang M H, Bao X Q, Zhang X J, Mu X, Lu K C, Li J H and Gao X X 2019 *J. Rare Earth.* **37** 393
[11] Sepehri-Amin H, Ohkubo T, Shima T and Hono K 2012 *Acta Mater.* **60** 819
[12] Ding G F, Guo S, Chen L, Di J H, Song J, Chen R J, Lee D and Yan A R 2018 *J. Alloys Compd.* **735** 795
[13] Ding G F, Liao S C, Di J H, Zheng B, Guo S, Chen R J and Yan A R 2020 *Acta Mater.* **194** 547
[14] Yan M, Jin J Y and Ma T Y 2019 *Chin. Phys. B* **28** 077507
[15] Zhou B B, Li X B, Cao X J, Yan G L and Yan A R 2016 *Chin. Phys. B* **25** 117504
[16] Lu K C, Bao X Q, Chen G X, Zhang X J, Tang M H, Mu X, Li J H and Gao X X 2019 *Scr. Mater.* **160** 86
[17] Knoch K G and Schneider G 1989 *IEEE Trans. Magn.* **25** 3426
[18] Hu Z H, Lian F Z, Zhu M G and Li W 2008 *J. Magn. Magn. Mater.* **320** 2364
[19] Arai S and Shibata T 1985 *IEEE Trans. Magn.* **21** 1952
[20] Sagawa M, Matsuura Y, Fujimura S, Yamamoto H and Hirosawa S 1985 *IEEE Trans. J. Magn. Jpn.* **1** 48
[21] Hirosawa S, Yamaguchi Y, Tokuhara K, Yamamoto H and Sagawa M 1987 *IEEE Trans. Magn.* **23** 2120
[22] Chen F G, Zhang L T, Jin Y and Cheng Y X 2018 *Mater. Charact.* **144** 547
[23] Lee M W, Bae K H, Lee S R, Kim H J and Jang T S 2017 *Arch. Metall. Mater.* **62** 1263
[24] Chen G X, Bao X Q, Lu K C, Lv X K, Ding Y, Zhang M, Wang C G and Gao X X 2019 *J. Magn. Magn. Mater.* **477** 17
[25] Lu K C, Bao X Q, Tang M H, Chen G X, Mu X, Li J H and Gao X X 2017 *Scr. Mater.* **138** 83
[26] Sepehri-Amin H, Liu L, Ohkubo T, Yano M, Shoji T, Kato A, Schrefl T and Hono K 2015 *Acta Mater.* **99** 297